



S-quinolin-2-yl-methyldithiocarbazate-based magnetic adsorbent for magnetic solid-phase extraction of heavy metals from water samples

Ahmad Jazmi Abdul Rahman, How N.-F Fiona, Mohd Hamzah Mohd Nasir, Sharifah Mohamad, Noorfatimah Yahaya, Maizatul Najwa Jajuli & Mazidatulakmam Miskam

To cite this article: Ahmad Jazmi Abdul Rahman, How N.-F Fiona, Mohd Hamzah Mohd Nasir, Sharifah Mohamad, Noorfatimah Yahaya, Maizatul Najwa Jajuli & Mazidatulakmam Miskam (2019): S-quinolin-2-yl-methyldithiocarbazate-based magnetic adsorbent for magnetic solid-phase extraction of heavy metals from water samples, International Journal of Environmental Analytical Chemistry, DOI: [10.1080/03067319.2019.1692827](https://doi.org/10.1080/03067319.2019.1692827)

To link to this article: <https://doi.org/10.1080/03067319.2019.1692827>



Published online: 26 Nov 2019.



Submit your article to this journal [↗](#)



Article views: 12



View related articles [↗](#)



View Crossmark data [↗](#)



S-quinolin-2-yl-methyldithiocarbazate-based magnetic adsorbent for magnetic solid-phase extraction of heavy metals from water samples

Ahmad Jazmi Abdul Rahman^a, How N.-F. Fiona^b, Mohd Hamzah Mohd Nasir^{c,d}, Sharifah Mohamad^e, Noorfatimah Yahaya^{d,f}, Maizatul Najwa Jajuli^a and Mazidatulakmam Miskam^a

^aSchool of Chemical Sciences, Universiti Sains Malaysia, Penang, Malaysia; ^bDepartment of Chemistry, Kulliyah of Science, International Islamic University Malaysia, Kuantan, Malaysia; ^cDepartment of Biotechnology, Kulliyah of Science, International Islamic University Malaysia, Kuantan, Malaysia; ^dCentral Research and Animal Facility (CREAM), Kulliyah of Science, International Islamic University Malaysia, Kuantan, Malaysia; ^eDepartment of Chemistry, University of Malaya, Kuala Lumpur, Malaysia; ^fIntegrative Medicine Cluster, Advanced Medical and Dental Institute (AMDI), Universiti Sains Malaysia, Bertam, Malaysia

ABSTRACT

New S-quinolin-2-yl-methyl-dithiocarbazate-based magnetic adsorbent (MNP-SQ2MDTC) for magnetic solid phase extraction (MSPE) was developed for the determination of Cd²⁺ and Cu²⁺ in water samples. The surface of MNP was first coated with (3-aminopropyl) triethoxysilane (APTES) as cross-linker and then SQ2MDTC incorporated covalently to the coated MNP. The newly prepared MNP-SQ2MDTC was analysed by Fourier Transform infrared (FT-IR), X-ray diffractometer (XRD), energy dispersive X-ray spectroscopy (EDX), vibrating-sample magnetometry (VSM), field emission scanning electron microscopy (FESEM), transmission electron microscopy (TEM) and Brunauer-Emmett-Teller (BET). Under optimal MSPE conditions (20 mg adsorbent dispersed in 25 mL of sample which adjusted to pH 6.0 and sonicated for 10 min, before desorbed in 0.5 mL of 1 M HClO₄ and sonicated for 5 min), the validation method revealed a good linearity (0.1–5.0 µg mL⁻¹) with the coefficient of determination (R²) in the range of 0.995–0.996 for the samples. The limits of detection (LOD) of the developed method for Cd²⁺ and Cu²⁺ were found to be 0.054 and 0.040 µg mL⁻¹, and limit of quantification (LOQ) were 0.180 and 0.134 µg mL⁻¹, respectively. The recoveries of Cd²⁺ ranged from 75.6% to 93.9% and from 81.5% to 98.7% for Cu²⁺. To the best of our knowledge, this is the first study that have investigated the use of magnetic nanoparticles coated SQ2MDTC for determination of Cd²⁺ and Cu²⁺ in water samples analysis based on complexation of the metal ions to the surface of amino groups.

ARTICLE HISTORY

Received 21 August 2019
Accepted 8 November 2019

KEYWORDS

Magnetic nanoparticles; Squinolin2ylmethyl-dithiocarbazate; heavy metals removal; magnetic solid phase extraction

1. Introduction

Heavy metal pollution is one of the most severe environmental problems, that occurred from both natural and anthropogenic sources. Due to the potential adverse effects of

these elements on humans, animals and ecosystems, the control and evaluation of the levels for different metals in diverse environmental, agricultural, food and clinical matrices are highly demanded by authorities and regulatory bodies [1,2]. For this reason, the development of sensitive and selective analytical procedures in order to determine metal ions have been a very active area of research.

Various methods have been applied for the heavy metal removals, such as electrochemical treatment technologies, membrane filtration, ion exchange, chemical precipitation and adsorption. Among the above methods, adsorption is considered as a high-profile method because of the considerable choice of adsorbent materials, operational ease and high efficiency [2–4]. However, the efficiency of adsorption processes relies on the performance of the adsorbents.

A wide variety of adsorbents have been applied to remove heavy metals, such as mesoporous silica [5,6], zeolites [7] and activated carbon [8]. However, these adsorbents inherited some drawbacks such as poor adsorption capacity, tedious separation process and poor recycling stability.

In order to eliminate the inherited drawbacks, surface modification of magnetic nanoparticle (MNP) is the prerequisite. Recent researches in magnetic separation led to the development of new materials which mostly focusing on the magnetic materials containing a magnetite core coated with silica ($\text{Fe}_3\text{O}_4/\text{SiO}_2$) [9,10] or polymer (Fe_3O_4 /polymer) [7,11]. The use of silica allows the introduction of the functional groups of interest, which is useful when surface changes are required. It increased the ease of modifying their surface functionality and their high surface area-to-volume ratio which can increase adsorption capacity and efficiency. MNP-based adsorbents can be easily recovered or manipulated from aqueous solutions under an external magnetic field due to their magnetic property. Hence, they have the advantages of simplicity, sensitivity and easy to operate in adsorption process [12,13]. They also have the potential to be used as a reusable adsorbent with convenient conditions. Although MNP-based adsorbents provide many advantages, they still suffer some drawbacks, i.e. sensitivity and selectivity. To overcome these limitations, intensive attempts have been made to improve the selectivity of magnetic adsorbents for the removal of heavy metals from environmental samples.

An extraction approach based on magnetic or magnetisable sorbents termed as magnetic solid-phase extraction (MSPE) was developed which is suitable for several analytes [14]. MSPE has vast advantages including ease of automation, high extraction efficiency and rapid phase separation [15]. It is one of the widely used methods currently due to its easiness, environmentally friendly and low cost [16]. Besides, no costly instrument or any type of device including column and cartridge is needed to operate MSPE, make it time-effective and easy to operate [17,18]. Recently, MSPE has been applied in various matrices for separation of pesticides [19–21], medicinal drugs [22,23], industrial chemicals [24,25] and dyes [26]. The use of MNP for the development of MSPE has become increasingly popular due to the advantages of easy control and simple separation.

A considerable interest has been shown in metal complexes of dithiocarbamate derivatives [27–29]. S-alkyl or aryl dithiocarbamates constitutes one of the most important classes of mixed hard-soft nitrogen–sulphur donor ligands [30], having four potential donor atoms of which two are sterically available at a time to chelate metal ions. In fact, the presence of hard nitrogen and soft sulphur atoms enable these ligands to react with both transition and main group metals [31]. Dithiocarbamate derivatives interact with

metal ions to give structures of different geometry and properties and they are often biologically active [32]. Different substitutions of *S*-alkyl and aryl dithiocarbazate have been explored such as *S*-methylthiocarbazate and *S*-benzylthiocarbazate. Many reports have been published on the successful formation of mentioned ligand, complexed with metals such as Ni(II) [33,34], Cu(II) [35,36], Cd(II) [27,37], Pb(II) [38] and Hg(II) [39]. Despite their excellent biological activities, the ability to form stable complexes with metal signifies great potential to be used for heavy metal removal.

In this work, MNP modified with *S*-quinolin-2-yl-methylthiocarbazate (SQ2MDTC) was designed for the adsorption of Cu^{2+} and Cd^{2+} as the model metals. The aim of this study is to prepare selective and sensitive magnetic adsorbents with excellent adsorption capacity with high magnetisation for easy regeneration. The influences of adsorption pH, adsorbent weight, sonication time, sample volume, type of eluent and eluent volume on the extraction capacity of the synthesised adsorbent were evaluated and discussed. The structure and surface properties of optimum MNP-SQ2MDTC were characterised.

2. Experimental

2.1. Chemicals and reagents

All chemicals and solvents used were of analytical reagent grade unless stated otherwise. Iron(III) chloride hexahydrate ($\text{FeCl}_3 \cdot 6\text{H}_2\text{O}$), ammonium iron(II) sulphate hexahydrate ($(\text{NH}_4)_2\text{Fe}(\text{SO}_4)_2 \cdot 6\text{H}_2\text{O}$), ammonia solution (NH_3) (28%), dichloromethane (CH_2Cl_2) and nitric acid (HNO_3) (65%) were purchased from QRëC® (Selangor, Malaysia). Potassium carbonate (K_2CO_3) and 3-aminopropyl triethoxysilane (APTES) was purchased from Sigma-Aldrich (USA). Carbon disulphide (CS_2) were obtained from Merck KGaA (Darmstadt, Germany). Hydrazine hydrate ($\text{NH}_2\text{NH}_2 \cdot \text{H}_2\text{O}$) (80% in water for synthesis) was obtained from Merck (Hohenbrunn, Germany). 2-chloromethylquinoline hydrochloride ($\text{C}_{10}\text{H}_8\text{ClN} \cdot \text{HCl}$) was purchased from Tokyo Chemical Industry Co., Ltd. (TCI) (Tokyo, Japan). Potassium hydroxide was purchased from Fisher Scientific (UK). Ethanol ($\text{CH}_3\text{CH}_2\text{OH}$) (absolute, denatured) which obtained from HmbG (Hamburg, Germany) was diluted to 40%, 80% and 90% for synthesis of SQ2MDTC. Dry toluene was prepared by adding 4 Å molecular sieves (Sigma-Aldrich, Inc., USA) into toluene ($\text{C}_6\text{H}_5\text{CH}_3$) (QRëC®, Selangor, Malaysia) at least 24 h before use.

2.2. Instrumentations

Fourier Transform-infrared (FT-IR) spectra were recorded using PerkinElmer Series 2000 FTIR spectrometer (USA) in the range of 400–4000 cm^{-1} . For the structural analysis, the XRD pattern was recorded using a monochromatised X-ray beam with nickel-filtered Cu K α radiation ($\lambda = 1.5419 \text{ \AA}$) at 40 mA and 40 kV on PANalytical X'Pert PRO MRD PW3040 X-ray diffractometer system (Almelo, Netherlands). The magnetic properties of the magnetic nanoparticles were determined using Lake Shore 7400 Series vibrating sample magnetometer system (USA). Quanta™ 650 FEG scanning electron microscope (SEM) (FEI, Holland) and Carl Zeiss energy filter transmission electron microscope (EFTEM) Libra® 120 (Oberkochen, Germany) were used to observe the size, morphology and structure of the nanoparticles. The surface area and pore size distribution of the MNP-SQ2MDTC were

measured by nitrogen adsorption–desorption isotherms at 77 K on Micromeritics ASAP 2020 (USA) using Brunauer–Emmett–Teller (BET) desorption methods. The magnetic solid phase extraction studies were performed on atomic adsorption spectrometer (AAS) (PerkinElmer AAnalyst™ 400, USA) and inductively coupled plasma–optical emission spectrometer (ICP–OES) (PerkinElmer Optima™ 8000, USA).

2.3. Preparation of magnetic adsorbents

2.3.1. Synthesis of Fe_3O_4 magnetic nanoparticles (MNP– Fe_3O_4)

MNP– Fe_3O_4 were prepared by co-precipitation method according to method done by Ali et al. [10] with minor modifications. 9.6 g $\text{FeCl}_3 \cdot 6\text{H}_2\text{O}$ and 4.8 g $(\text{NH}_4)_2\text{Fe}(\text{SO}_4)_2 \cdot 6\text{H}_2\text{O}$ (ratio 2:1) were added to 120 mL distilled water under nitrogen atmosphere and then stirred for 5 min at 60°C. Then, 90 mL of ammonia solution (8 M) was added dropwise into the reaction mixture. A black precipitate was formed immediately, and the reaction was allowed to proceed for another one hour. Then, by using an external magnet, MNP– Fe_3O_4 was collected before it was washed with excess doubly hot distilled water until neutral pH was obtained. Finally, the product was dried under vacuum at 60°C for 24 h.

2.3.2. Synthesis of silica core-shell magnetic nanoparticles (MNP–APTES)

Silica core–shell Fe_3O_4 MNP were done in the same manner as previously reported by Rajabi et al. [40]. First, 5 g of freshly prepared Fe_3O_4 MNP and 20 mL of dry toluene were sonicated for 30 min. Then, 4.68 mL APTES reagent was added to the sonicated mixture and stirred under nitrogen atmosphere at 60°C for 12 h. After that, the mixture was cooled down before the precipitates were magnetically separated and washed with dry toluene and water–acetone mixture (20:80% v/v). The functionalised Fe_3O_4 MNP will further be dried under vacuum for 24 h at ambient temperature.

2.3.3. Synthesis of *S*-quinolin-2-yl-methyldithiocarbazate (SQ2MDTC)

70 mL of 90% ethanol was filled in a beaker before 0.4 mol of potassium hydroxide was dissolved and mixed with 0.2 mol of hydrazine hydrate. The mixture was then placed in an ice salt bath to cool to 0°C. Carbon disulphide (0.2 mol) was added dropwise with temperature below –8°C and constantly stirred for about 1 h. Two layers were formed from the reaction and separated in different beakers. Then, 60 mL of 40% ethanol was added to the lower layer of brown oil. The mixture was then kept in an ice bath. 2-chloromethylquinoline hydrochloride (0.2 mol) was dissolved in 80 mL of 80% ethanol before added dropwise to the mixture with vigorous stirring. A cream-coloured product which is *S*-quinolin-2-yl-methyl-dithiocarbazate will be formed. The product was filtered, recrystallised with ethanol and dried *in vacuo* over silica gel.

2.3.4. Synthesis of MNP functionalised with *S*-quinolin-2-yl-methyldithiocarbazate (MNP–SQ2MDTC) adsorbent

MNP–SQ2MDTC was prepared according to a method previously reported by Mohammadi et al. [41]. About 1 g of MNP–APTES and 0.07 g potassium carbonate was dispersed in 50 mL dry toluene and mechanically stirred for 30 min. Subsequently, 1 g of SQ2MDTC was added and was kept under mechanical stirring at 60°C for 24 h. Then, the final

product was removed by magnetic decantation and washed twice by dry dichloromethane and water, respectively, to remove the unattached substrates. The product was dried under vacuum for 24 h at ambient temperature and kept over the silica gel.

2.4. Magnetic solid phase extraction (MSPE) procedure

A portion of sample containing the analyte ions was transferred into a 50 mL beaker and adjusted to pH 6.0 with 0.1 mol L⁻¹ HNO₃ and 0.1 mol L⁻¹ aqueous ammonia. Then, 20 mg of MNP-SQ2MDTC were added and dispersed by ultrasonication for 10 min at room temperature to facilitate the metal ions adsorption process. A strong external magnet was used to separate the magnetic adsorbent and the supernatants were decanted. Next, 0.5 mL of 1.0 mol L⁻¹ perchloric acid was used to desorb the adsorbed analytes from the isolated adsorbent and sonicated for 5 min. Finally, the adsorbent was separated by external magnet again and the eluate was introduced into AAS for subsequent analysis.

2.5. Method validation

To validate the developed MSPE method, its linearity, precision, limit of detection (LOD), limit of quantification (LOQ) and accuracy were studied under optimised conditions. The linearity was determined through the standard curves of working solutions at concentration ranging between 0.1 µg mL⁻¹ to 5 µg mL⁻¹. Each sample was prepared by diluting the standard solution of specific metal ion with deionised water and was examined by triplicate analysis. The calibration curves were prepared using five spiking levels of analytes.

LOD was calculated according to IUPAC definition where the limit of detection is equal to three times of standard deviation and divided by the slope of method calibration curve ($LOD = 3 \times SD_{\text{blank}}/m, n=3$). For the limit of quantification, it was 10 times of standard deviation and divided by the slope of method calibration curve ($LOQ = 10 \times SD_{\text{blank}}/m, n=3$).

The assessment of precision expressed as relative standard deviation (RSD) was done in term of repeatability (intra-day) and reproducibility (inter-day). The intra-day precisions were calculated from six parallel procedures performed in a single day, while the inter-day precisions were measured over three consecutive days.

2.6. Real sample analysis

The performance of proposed method has been investigated by applying in real water samples collected from various local rivers. The obtained samples were filtered through filter paper and adjusted to pH 6.0 with 0.1 mol L⁻¹ HNO₃ and 0.1 mol L⁻¹ aqueous ammonia. Then, unspiked and spiked samples (0.1 µg mL⁻¹ for Cu²⁺ and 1.0 µg mL⁻¹ for Cd²⁺) were prepared before metal ions were extracted using synthesised adsorbent in optimised MSPE conditions. The eluents were analysed using ICP-OES in triplicate measurements.

3. Results and discussion

3.1. Synthesis of MNP functionalised with *S*-quinolin-2-yl-methyldithiocarbazate (MNP-SQ2MDTC) adsorbent

In this study, MNP-SQ2MDTC has been successfully synthesised prior to complex formation with heavy metals. As illustrated in Figure 1, core-shell structured Fe_3O_4 -SQ2MDTC composites were readily prepared and subsequently employed to form complex with heavy metals. In the first step, the chemical co-precipitation of Fe^{2+} and Fe^{3+} ions in ammonia solution afforded the magnetite nanoparticles. The co-precipitation process was carried out in a nitrogen atmosphere at 60°C to avoid the oxidation of the magnetic

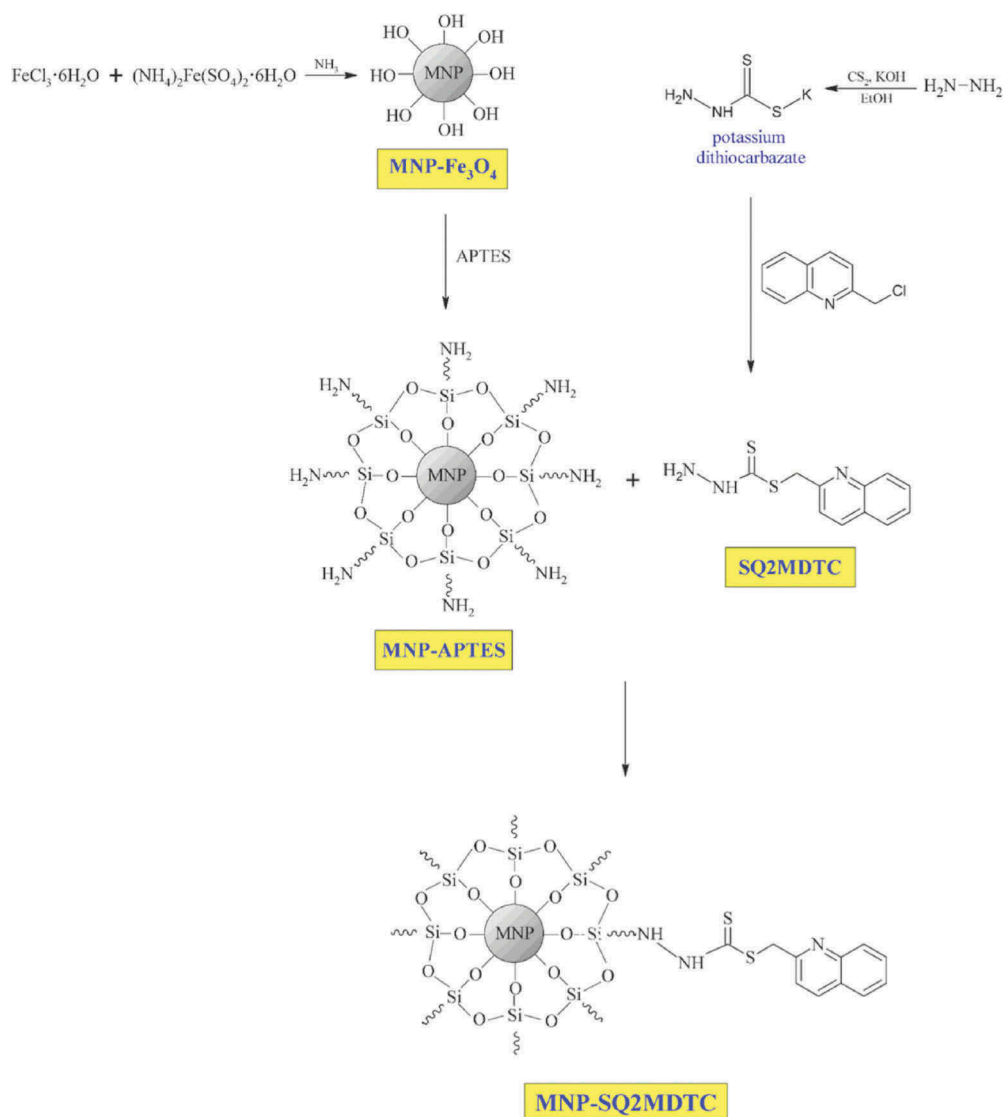


Figure 1. Schematic of the synthesis of MNP-SQ2MDTC.

core shell. Immediately after the completion of the process, an aqueous solution of ammonia was added in order to precipitate and produce MNP.

The SQ2MDTC ligand was synthesised by the addition of hydrazine hydrate and carbon disulphide in ethanolic potassium hydroxide at 0°C. Two distinctive layers were formed and separated to obtain the lower brown layer of potassium dithiocarbazate. Then, chloromethylquinoline hydrochloride was added and the positive-charged potassium on potassium dithiocarbazate was substituted with chloromethylquinoline to form cream colour SQ2MDTC precipitate. The ligand was prepared with several modifications to optimise the yield as compared to the work previously reported by How et al. [30]. The concentration of potassium hydroxide has been doubled to increase the basicity of the solution which will increase the reaction rate between hydrazine hydrate and carbon disulphide to form potassium dithiocarbazate.

APTES was added to the MNP in order to reduce the agglomeration and as crosslinker to provide active site for SQ2MDTC attachment. SQ2MDTC possesses both hard nitrogen and soft sulphur donor atoms; hence, it can bind either with hard atoms or soft atoms [33,42,43]. In addition, MNP-APTES can be classified as 'hard' due to abundance of oxygen and silica atoms on its surface. Thus, theoretically, nitrogen atom of SQ2MDTC is more favourable to bind with MNP-APTES since hard atom will only bind with other hard atoms. Potassium carbonate (K_2CO_3) was used in the synthesis of MNP-SQ2MDTC to activate MNP-APTES and improve the conjugation process of SQ2MDTC to MNP [44].

3.2. Characterisation of MNP-SQ2MDTC

3.2.1. FT-IR analysis

The FTIR spectra for the prepared magnetic adsorbents are shown in Figure 2. For Fe_3O_4 magnetic nanoparticles (Figure 2(a)), a stretching vibration at 3392 cm^{-1} was assigned for the O–H bonds on the surface iron atoms. The bands at low wave numbers ($\leq 700\text{ cm}^{-1}$) signified the vibrations of Fe–O bonds of iron oxide, Fe_3O_4 , in which the peaks at 634 and 583 cm^{-1} were assigned to the $Fe^{3+}-O-Fe^{3+}$ and $Fe^{2+}-O-Fe^{2+}$ symmetrical stretching vibrations, respectively. It should be pointed out that the band around 1624 cm^{-1} was attributed to the bending vibration of H–O–H linkage of water in the Fe_3O_4 nanoparticles.

The introduction of APTES coating on the surface of MNP was confirmed by the existence of several bands in the spectrum of MNP-APTES (Figure 2(b)). The bands at 1110 and 1021 cm^{-1} were assigned to SiO–H and Si–O–Si groups. The bands at 893 and 798 cm^{-1} were ascribed as the stretching Si–O–H and vibration of OH on the surface of MNP. The broad bands at 1620 and 3406 cm^{-1} were assigned to N–H stretching vibration and bending mode of free –NH₂ group, respectively. The appearance of two bands at 2926 and 2853 cm^{-1} indicated the symmetric and asymmetric C–H₂ stretching vibration, respectively, which confirmed the anchoring of propyl group on the surface of MNP.

For SQ2MDTC spectrum (Figure 2(c)), a sharp band at 3283 cm^{-1} is the most significant as it indicates the presence of N–H bond. NH₂ rocking mode can also be found at 1049 cm^{-1} , while NH₂ stretching band can be found at 972 cm^{-1} . Bands at 762 cm^{-1} , 476 cm^{-1} and 437 cm^{-1} were assigned as bending N–C–S [32]. The medium band at 995 cm^{-1} is due to –CSS stretching vibration. The C–S band can be found at 828 cm^{-1} . For the aryl group, bands between 1400 and 1650 cm^{-1} have been assigned to C–C and C = C stretching modes. The observed stretching band appeared at 1566 cm^{-1} has been

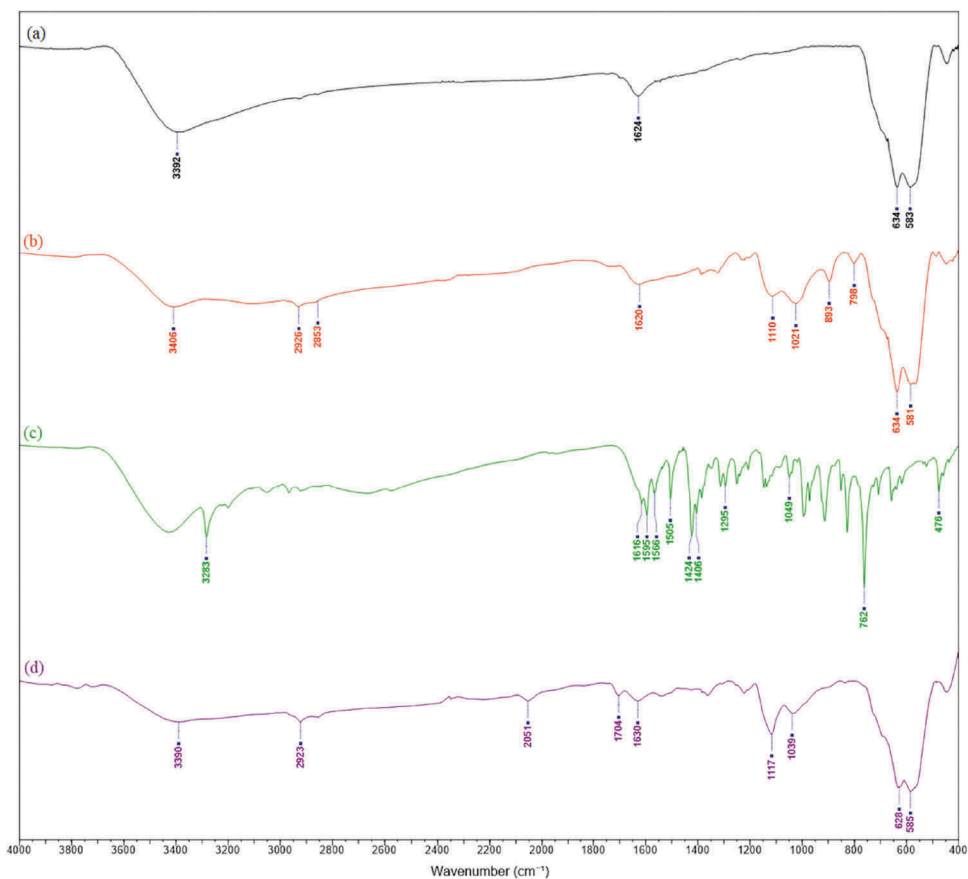


Figure 2. FT-IR spectra of (a) MNP- Fe_3O_4 , (b) MNP-APTES, (c) SQ2MDTC, and (d) MNP SQ2MDTC.

assigned to C–C stretching vibrations. Bands at 1595 and 1616 cm^{-1} were attributed as C = C stretching bonds. The medium bands at 1505 and 1295 cm^{-1} were assigned to C = N and C–N stretching modes, respectively.

Following the functionalisation of MNP-APTES with SQ2MDTC ligand, the resultant product showed two new prominent bands at 2051 and 1704 cm^{-1} (Figure 2(d)), which both are assigned as the stretching vibrations of C = N. Other peaks were similar to the peaks in MNP-APTES spectrum. This indicates that the NH_2 of the ligand has been successfully bonded to methyl group of APTES. These results confirmed that the MNP-SQ2MDTC has been successfully synthesised.

3.2.2. X-ray diffraction analysis

XRD is a powerful instrument for recognition of crystalline structure of synthesised materials. The XRD patterns of (i) MNP- Fe_3O_4 , (ii) SQ2MDTC and (iii) MNP-SQ2MDTC were depicted in Figure 3(a). The 2θ peaks at 30.1° , 35.4° , 43.1° , 52.8° , 57.3° and 63.3° corresponded indicating (220), (311), (400), (422), (511) and (440), respectively. The position and relative intensities of all diffraction signals of the both samples matched well with the characteristic peaks of standard pattern of standard iron oxide (Fe_3O_4) diffraction data

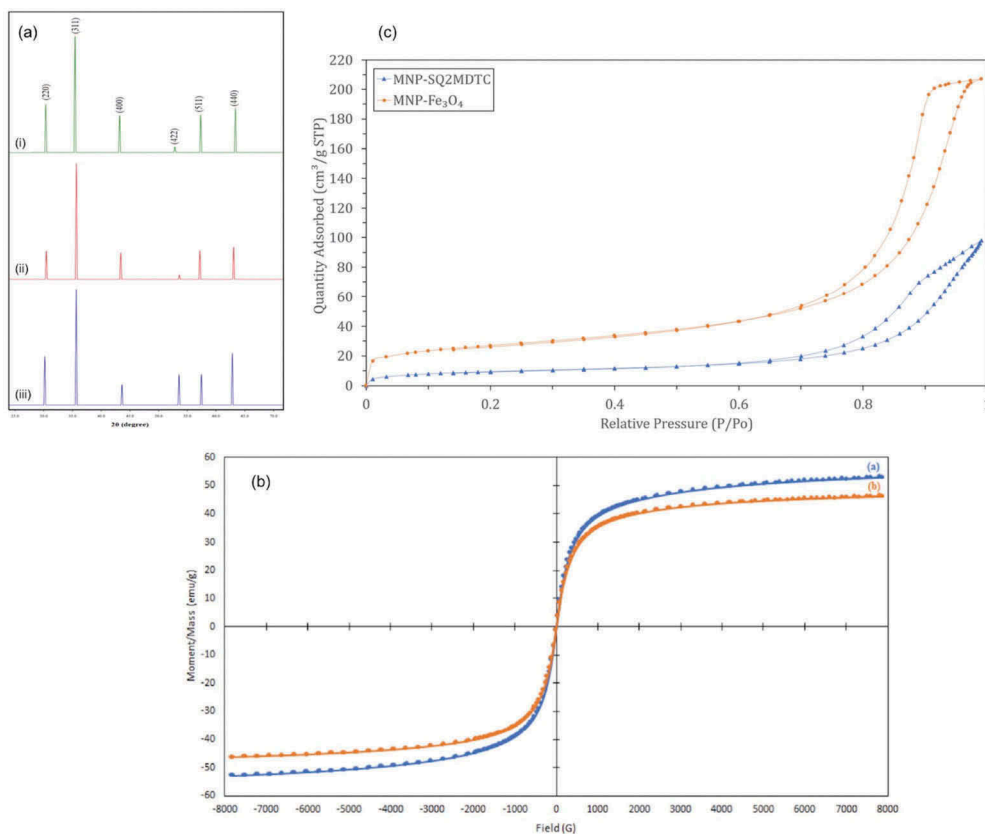


Figure 3. (a) XRD patterns of (i) MNP- Fe_3O_4 , (ii) MNP-APTES, and (iii) MNP-SQ2MDTC, (b) Hysteresis loops of (i) MNP- Fe_3O_4 and (ii) MNP-SQ2MDTC and (c) N_2 adsorption isotherms of MNP- Fe_3O_4 and MNP-SQ2MDTC.

(ICSD No. 01-075-0449). These results indicated that the immobilisation process did not change the magnetic crystalline profile as reported in several literatures [45,46]. It was also revealed that the synthesised materials have cubic spine structures.

3.2.3. Vibrating sample magnetometry analysis

Strong magnetisation is of great importance for the separation of target analytes through MSPE process. To investigate the magnetic properties of synthesised materials, the hysteresis loops were measured with a VSM. Figure 3(b) shows the magnetisation curves of MNP- Fe_3O_4 and MNP-SQ2MDTC. No hysteresis was observed in the hysteresis loops of both materials and the remanence and coercivity were nearly zero, exhibiting typical superparamagnetic behaviour. It is crucial for magnetic nanoparticles to have superparamagnetic property to prevent aggregation and allow the nanoparticles to re-disperse rapidly when the magnetic field was removed [47]. The saturation magnetisation (M_s) of MNP- Fe_3O_4 and MNP-SQ2MDTC were 52.985 emu/g and 46.353 emu/g, respectively. MNP-SQ2MDTC has lower saturation magnetisation than the bare MNP. This indicates that the size of MNP-SQ2MDTC has increased due to the coating of silica and the

SQ2MDTC. As MNP-SQ2MDTC has high M_s (compared to the minimum of 16.3 emu/g) [10], it can be easily collected by permanent magnets in a very short time duration.

3.2.4. Brunauer-Emmett-Teller (BET) analysis

The N_2 adsorption isotherms of MNP- Fe_3O_4 and MNP-SQ2MDTC are depicted in Figure 3(c). The samples exhibit type IV isotherms and a typical adsorption isotherm with H1 hysteresis, according to the IUPAC classification, associated with the presence of mesopores. The p/p_0 position of the inflection greater than 0.8, indicates the structural (porous) characteristic and the sharpness of the step indicates the uniformity of the mesopore size distribution [48].

Based on BJH pore size distribution, the synthesised MNP-SQ2MDTC was mesoporous material with the specific surface area was found to be 33.52 m^2/g , total pore volume of 0.144 cm^3/g and mean pore diameter of 17.22 nm. The effective attachment of SQ2MDTC in the MNP-APTES pores is evidenced by the expressive reduction of the surface area and pore volume [48], as presented in Table 1. The binding of significant amount of SQ2MDTC on MNP-APTES altered the textural morphologies; it means that the SQ2MDTC may occupy a volume inside the pores of the silica nanocomposite and, as a result, a decrease in the pore volume was observed.

3.2.5. FESEM analysis

The morphology of the synthesised MNP- Fe_3O_4 and MNP-SQ2MDTC were examined by using FESEM analysis. Figure 4 reveals that both materials have uniform spherical morphology and homogeneous particle size distribution. It can be seen that most of the particles formed were nanometre-sized where MNP- Fe_3O_4 has an average diameter of about 17 nm and MNP-SQ2MDTC has an average diameter of 35 nm. The size increment may be due to the addition of SQ2MDTC ligand on the surface of MNP.

3.2.6. TEM analysis

Transmission electron microscopes (TEM) is a powerful instrument which generates highly magnified image by employing a high voltage electron beam through the specimen. Therefore, it has been used for analysis of particle shapes and morphologies. Figure 4(c-d) shows the TEM micrographs of MNP- Fe_3O_4 and MNP-SQ2MDTC. It can be seen that both nanomaterials have almost uniform and distinguishable polygonal shapes. However, MNP-SQ2MDTC appears darker compared to MNP- Fe_3O_4 , which indicates MNP-SQ2MDTC has a higher density than MNP- Fe_3O_4 [49]. Both MNP- Fe_3O_4 and MNP-SQ2MDTC also exhibit relatively good monodispersity. The average diameter of MNP- Fe_3O_4 and MNP-SQ2MDTC are 11.25 nm and 13.71 nm, respectively. It is common for the coated MNP to have the increment of diameter in the range of 0–5 nm compared to the naked MNP [50] and MNP-SQ2MDTC has a bigger size due to the attachment of SQ2MDTC ligand on the surface of MNP.

Table 1. BET surface area of MNP- Fe_3O_4 and MNP-SQ2MDTC.

	MNP- Fe_3O_4	MNP-SQ2MDTC
BET specific surface area (m^2/g)	94.8458	33.5171
Mean pore volume (cm^3/g)	0.319	0.144
Mean pore diameter (nm)	13.4907	17.2217

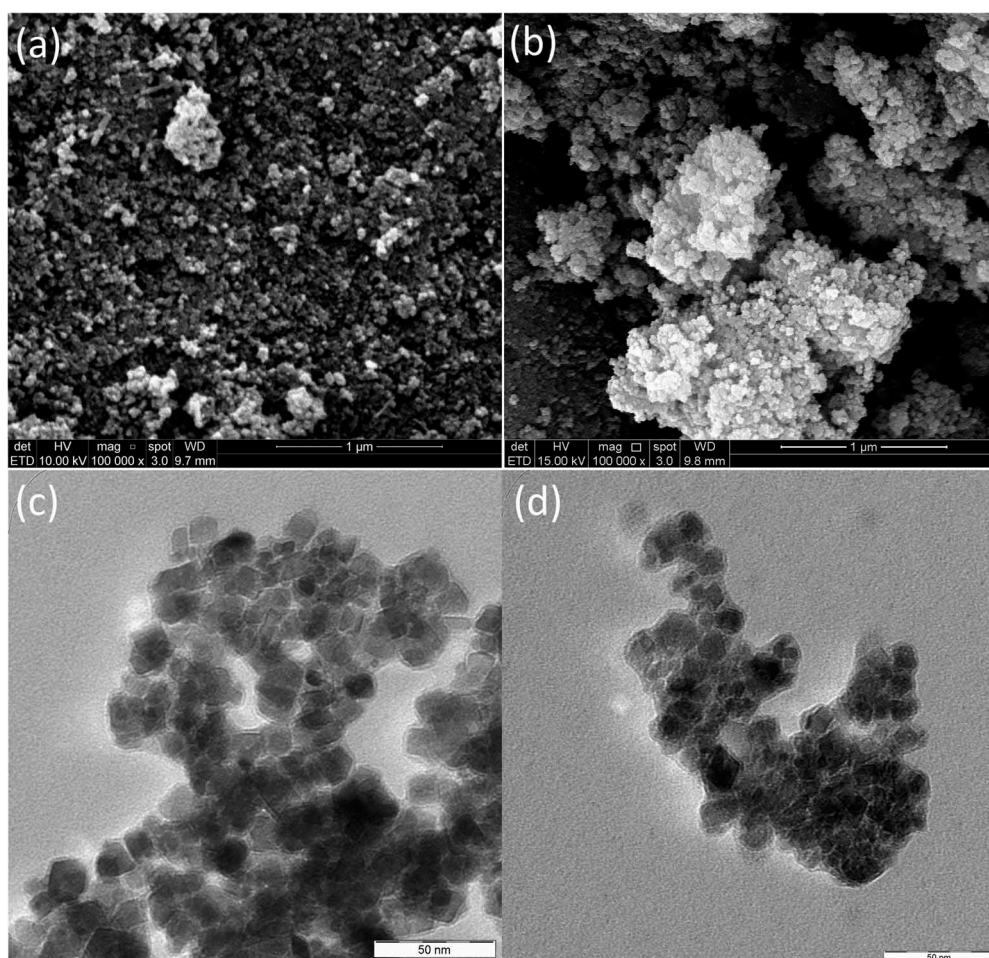


Figure 4. SEM images of (a) MNP- Fe_3O_4 and (b) MNP-SQ2MDTC, TEM micrographs of (c) MNP- Fe_3O_4 and (d) MNP-SQ2MDTC.

3.3. Optimisation of parameters affecting MSPE procedure

3.3.1. Sample pH

The aqueous pH has a vital role in the MSPE as it could enhance the efficiency of heavy metals adsorption, influencing surface chemistry, reduce interference from the matrix, determining the adsorbent surface charge and the degree of ionisation and speciation of the adsorbed metal ions [51–53]. The effect of pH on the adsorption percentage of metal ions was studied with pH varying from 3 to 6. The pH was adjusted by utilising diluted acid or base (0.1 M HCl or 0.1 M NaOH). As could be seen from Figure 5(a), the quantitative adsorption for both Cd^{2+} and Cu^{2+} were increased gradually from low pH and reach maximum (>90%) at pH 6. This may due to the competition of metal ions and hydrogen ions to attach at binding site at low pH levels (i.e. pH 2–3) [10]. In contrast, more metal ions are binded to the adsorbent and successfully extracted from water at higher pH (i.e. pH 6). Moreover, in acidic media, the structure of the attached SQ2MDTC ligand might have

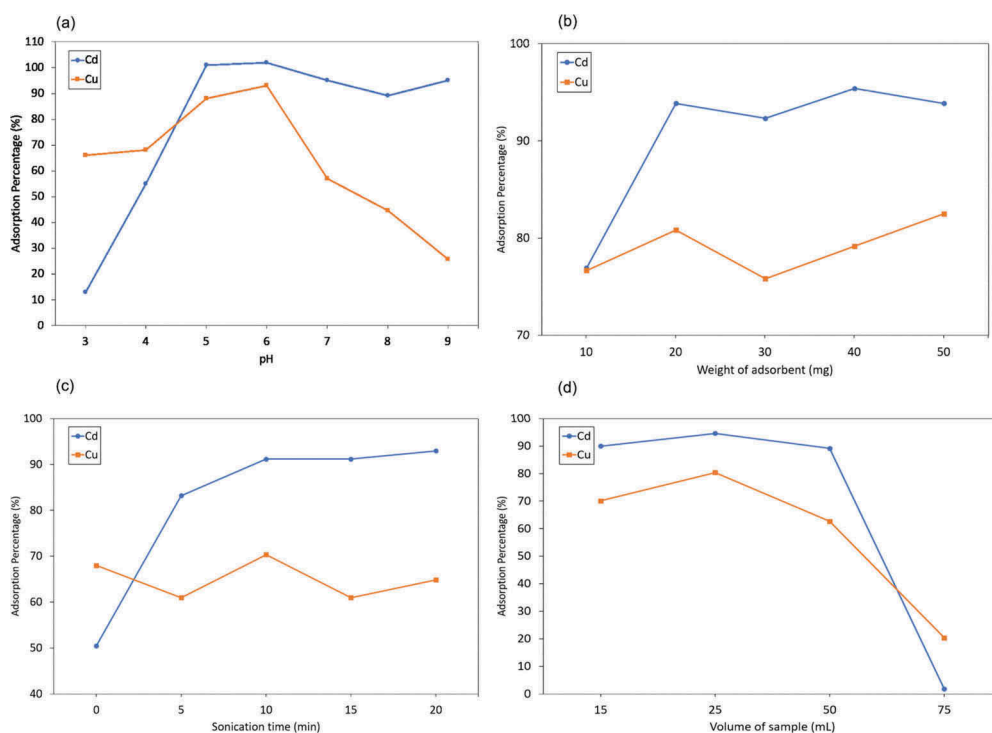


Figure 5. Effect of (a) pH (b) adsorbent weight (c) sonication time and (d) volume of sample on the adsorption percentage of Cd²⁺ and Cu²⁺ ions. MSPE conditions: Cd²⁺ and Cu²⁺ ions concentration: 100 $\mu\text{g L}^{-1}$, sonication time for adsorption: 5 min; desorption eluent: HCl, volume of eluent: 5 mL, sonication time for desorption: 10 min.

been affected, where the nitrogen atoms could be protonated and the S–H group could be oxidised, resulting in instability and incomplete formation of ligand-metal ion complex [54–56]. Conversely, the precipitation of metal ions as hydroxides could happen at high alkaline pH value beyond a pH of 6 [10,57]. The complexes between adsorbent and metal ions unlikely to be formed; hence, the preconcentration on the adsorbent is not favoured [58]. Considering this reason, extraction of metal ions at pH above 6 was not studied further. Hence, pH 6 was selected for all subsequent experiments in this work.

3.3.2. Weight of adsorbent

Nanoparticles have significantly higher surface area and shorter diffusion route compared with other sorbents. These can result in high extraction efficiency and fast extraction dynamics [59]. Thus, satisfactory results with less adsorbent can be achieved with these sorbents. In order to investigate the optimum amount of adsorbent needed for the extraction of target analytes, the amount of MNP-SQ2MDTC adsorbent was varied from 10 to 50 mg. Based on the results obtained (Figure 5(b)), it can be seen that the high percentage of adsorption for adsorbent weight more than 20 mg (75–80% for Cu²⁺ and 92–95% for Cd²⁺). Thus, 20 mg was selected as optimum weight and utilised for the subsequent analysis.

3.3.3. Adsorption sonication time

The duration of sonication during adsorption process was varied to determine the optimum reaction time and minimise the required time to process each sample. Different sonication time for adsorption was investigated at 0, 5, 10, 15 and 20 min. As depicted in Figure 5(c), 10 min provided the highest adsorption percentage of Cd^{2+} and Cu^{2+} . As the sonication time increased to 20 min, there is no significant increment for Cd^{2+} . Thus, 10 min was employed during adsorption process.

3.3.4. Sample volume

The maximum applicable sample volume should be determined to explore the probability of enriching low concentration of analyte from large volume. The sample volume of 15, 25, 50, 75 and 100 mL were tested for this purpose. As shown in Figure 5(d), the best results were given by sample volume of 25 mL which are 80.37% (Cu^{2+}) and 94.57% (Cd^{2+}). Thus, 25 mL was chosen as the optimum sample volume.

3.3.5. Type and volume of eluent

In order to achieve high enrichment factor, desorption solvents were varied for the desorption studies. Different acidic mediums were tested as they are more favourable for metal ions desorption [10]. The result is shown in Figure 6(a) indicated that 1 M perchloric acid (HClO_4) was efficient as the desorption eluent for both Cu^{2+} and Cd^{2+} . Moreover, metals like Cu^{2+} and Cd^{2+} are effectively desorbed with a strong acid [60,61], and HClO_4 is one of the strongest Brønsted–Lowry acids where its $\text{p}K_a$ value (< -10) is the lowest among the acid tested. Therefore, HClO_4 has been adopted as eluent. The effect of HClO_4 volume was investigated in the range of 0.5–30 mL. Based on the results in Figure 6(b), the HClO_4 volume of 0.5 mL gives the best result and was the lowest volume for the desorption process. Thus, a volume of 0.5 mL of 1 M HClO_4 was selected for the next procedure.

3.3.6. Desorption sonication time

The desorption times are also important for the recovery of Cu^{2+} and Cd^{2+} using MNP-SQ2MDTC adsorbent. Sonication method was deployed to aid the desorption process. Hence, the duration of sonication was varied from 5 to 15 min to determine the most optimised time. Experimental results (Figure 6(c)) shows that a good recovery was obtained at 5 to 10 min. Hence, it can be concluded that 5 min are sufficient enough to achieve the maximum recovery.

3.4. Analytical performance

Under the optimised experimental conditions, the newly synthesised MSPE adsorbent showed good linearity in the calibration range of 0.1–5.0 $\mu\text{g mL}^{-1}$, with coefficient of determination (R^2) of 0.9952 and 0.9964 for Cd^{2+} and Cu^{2+} , respectively. The limit of detection (LOD) for extraction of Cd^{2+} and Cu^{2+} were found to be 0.207 and 0.019 $\mu\text{g mL}^{-1}$, and their limit of quantification (LOQ) were 0.690 and 0.064 $\mu\text{g mL}^{-1}$, respectively. The intra-day RSD of Cd^{2+} and Cu^{2+} were 3.01% and 1.48%, and the inter-day RSD of Cd^{2+} and Cu^{2+} were 4.54% and 0.66%, respectively. Table 2 summarises the analytical performance of the established method. Table 2 summarises the analytical performance of the established method.

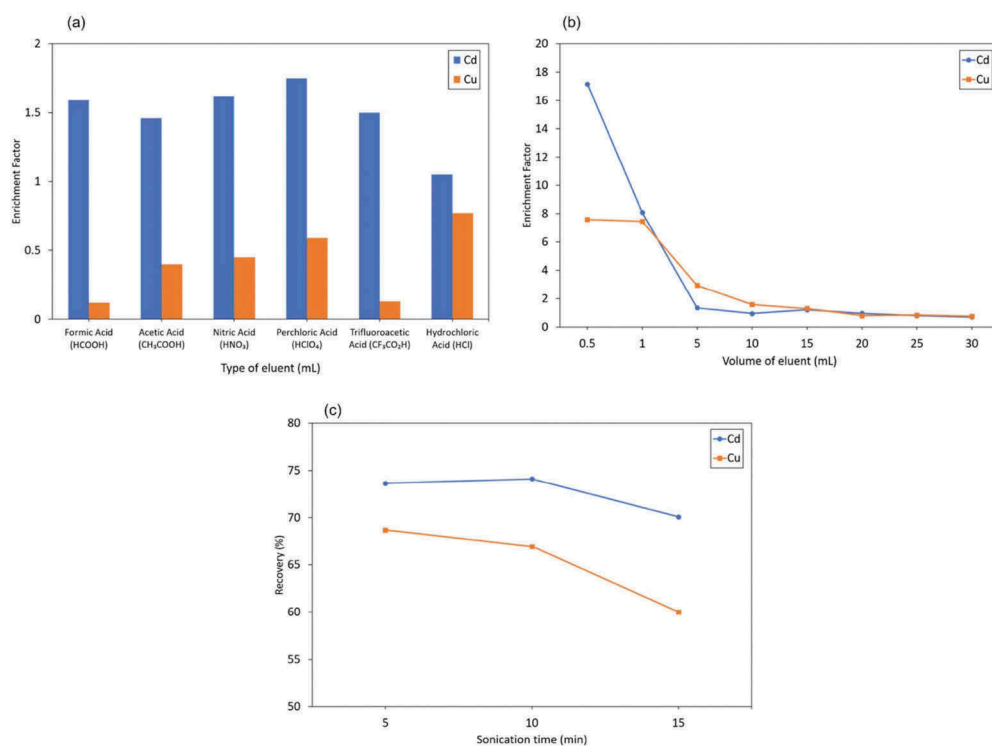


Figure 6. Effect of (a) different type of eluent (b) eluent volume on enrichment factors of Cd²⁺ and Cu²⁺ ions on enrichment factor and (c) desorption sonication time on the recovery percentage of Cd²⁺ and Cu²⁺ ions. MSPE conditions: Cd²⁺ and Cu²⁺ ions concentration: 100 µg L⁻¹, volume of sample: 25 mL, pH: 6, sonication time for adsorption: 10 min, mass of adsorbent: 20 mg.

Table 2. Validation parameters for the proposed method for Cd²⁺ and Cu²⁺.

Analytes	Linearity range (µg mL ⁻¹)	coefficient of determination (R ²)	LOD (µg mL ⁻¹)	LOQ (µg mL ⁻¹)	Intra-day RSD (% , n = 6)	Inter-day RSD (% , n = 3)
Cd ²⁺	0.1–5.0	0.995	0.054	0.180	3.01	4.54
Cu ²⁺	0.1–5.0	0.996	0.040	0.134	1.48	0.66

3.5. Analytical application on real sample

In order to evaluate the accuracy and applicability, the proposed extraction method has been applied in environmental samples for the determination of Cd²⁺ and Cu²⁺ speciation. The analytical results along with the recoveries for the unspiked and spiked samples with known concentration are listed in Table 3. It can be seen from the obtained results that the overall recoveries for Cd²⁺ were in the range of 75.6% to 93.9%, while for Cu²⁺, the recoveries ranged from 81.5% to 98.7% for Cu²⁺. The recoveries of both analytes obtained RSD values lower than 0.68% for both Cd²⁺ and Cu²⁺, which indicated a precise method.

3.6. Method performance comparison

The performance of developed MSPE method has been reviewed by a comparison with other reported preconcentration techniques in literature, as summarised in Table 4. It

Table 3. Analytical results for determination of cadmium and copper in different water samples (mean \pm SD, $n = 3$) using the MSPE procedure.

Sample	Element	Added ($\mu\text{g mL}^{-1}$)	Found ($\mu\text{g mL}^{-1}$)	Recovery (%)
River 1	Cu	0	0.662 \pm 0.002	-
		0.1	0.710 \pm 0.002	93.2
	Cd	0	0.120 \pm 0.002	-
River 2	Cu	0	0.676 \pm 0.002	-
		0.1	0.766 \pm 0.001	98.7
	Cd	0	0.119 \pm 0.002	-
River 3	Cu	0	0.334 \pm 0.003	-
		0.1	0.636 \pm 0.003	82.8
	Cd	0	0.124 \pm 0.001	-
River 4	Cu	0	0.376 \pm 0.005	-
		0.1	0.694 \pm 0.002	81.5
	Cd	0	0.120 \pm 0.001	-
River 5	Cu	0	0.973 \pm 0.004	86.9
		0.1	0.630 \pm 0.001	-
	Cd	0	0.706 \pm 0.000	96.7
		0	0.116 \pm 0.002	-
		1.0	0.844 \pm 0.004	75.6

Table 4. Method performance comparison for determination of Cd^{2+} and Cu^{2+} in various sample matrices.

Pretreatment technique	Sample matrix	Analyte	LOD ($\mu\text{g mL}^{-1}$)	Reference
Ionic liquid based dispersive liquid-liquid microextraction (IL-DLLME)	Sea water, lake water, stream water, tap water	Cu	0.81	[62]
Ultrasound-assisted emulsification solidified floating organic drop microextraction (USAE-SFODME)	Drinking water, sea water, river water	Cu	0.76	[63]
Cloud-point extraction (CPE)	Mineral water, tap water, sea water	Cd	0.15	[64]
Solid phase extraction (SPE)	Leakage water, tap water, drain water	Cd	0.07	[65]
Magnetic solid phase microextraction (MSPME)	Sugar can spirit	Cu	0.032	[66]
Magnetic solid phase extraction (MSPE)	Water	Cd	0.038	
		Cu	0.040	This work
		Cd	0.054	

was evident that the proposed method in the current work produced acceptable results and in the range with other methods. Liquid phase microextraction methods including ionic liquid-based dispersive liquid-liquid microextraction (IL-DLLME) and ultrasound-assisted emulsification solidified floating organic drop microextraction (USAE-SFODME) have been developed recently to remove Cu from water, but they produced higher LODs compared to the presented MSPE method. Vatankhah et al. [64] opted for a greener method which is cloud point extraction (CPE) for the separation and pre-concentration of cadmium and lead ions, but the LOD obtained of cadmium is two times higher than this reported work. The traditional solid phase extraction (SPE) method also has been used recently by Topuz, Kabadayi and Solmaz [65] for determination of several heavy metals including Cd, where they obtained a slightly higher LOD than current method. However, SPE technique is known to have several disadvantages including tedious steps, requires costly extraction device, and usually having column blockage and high back pressure problems. A new miniaturised technique called magnetic solid phase microextraction (MSPME) has been applied by Meira et al. [66]

for the determination of Cu, Cd, Pb and V in Brazilian sugarcane spirit. This method obtained LOD lower than the MSPE method proposed in this report, but the procedure is time consuming as drying process at ambient temperature is required after extraction prior instrument analysis. The reusability of the material is also questionable as no desorption process proposed. Generally, the MNP-SQ2MDTC-based MSPE we propose has a good performance with a relatively low LOD, along with several eminent merits including simple and rapid extraction, cost effective and high efficiency.

4. Conclusion

The new MNP functionalised with 5-quinolin-2-yl-methyldithiocarbazate (MNP-SQ2MDTC) were successfully synthesised and developed as an adsorbent to remove Cd^{2+} and Cu^{2+} from aqueous samples prior to determination using ICP-OES. The MNP-SQ2MDTC-based MSPE has a high adsorption capacity, a better sensitivity, and good accuracy and precision. It has the potential to be applied in the removal of Cd^{2+} and Cu^{2+} in the environmental waters. It also provides a simple and rapid extraction for heavy metals.

Disclosure statement

No potential conflict of interest was reported by the authors.

Funding

This work was supported by funding from Universiti Sains Malaysia Research Grants (Short Term: 304.PKIMIA.6313334; Bridging: 304.PKIMIA.6316492) and International Islamic University Malaysia Research Initiative Grants (RIGS15-136-0136, P-RIGS18-029-0029).

ORCID

Noorfatimah Yahaya  <http://orcid.org/0000-0002-3079-7837>

References

- [1] S. Chowdhury, M.A.J. Mazumder, O. Al-Attas and T. Husain, *Sci. Total Environ.* **476**, 569 (2016).
- [2] J. Xu, Z. Cao, Y. Zhang, Z. Yuan, Z. Lou, X. Xu and X. Wang, *Chemosphere* **195**, 351 (2018). doi:10.1016/j.chemosphere.2017.12.061.
- [3] A.I.A. Sherlala, A.A.A. Raman, M.M. Bello and A. Asghar, *Chemosphere* **193**, 1004 (2018). doi:10.1016/j.chemosphere.2017.11.093.
- [4] I. Ali, *Chem. Rev.* **112**, 5073 (2012). doi:10.1021/cr300133d.
- [5] Y.J. Acosta-Silva, R. Nava, V. Hernández-Morales, S.A. Macías-Sánchez, M.L. Gómez-Herrera and B. Pawelec, *Appl. Catal. B Environ.* **110**, 108 (2011). doi:10.1016/j.apcatb.2011.08.032.
- [6] W. Xie and X. Zang, *Food Chem.* **194**, 1283 (2016). doi:10.1016/j.foodchem.2015.09.009.
- [7] S.N.A. Baharin, N. Muhamad Sarih, S. Mohamad, S. Shahabuddin, K. Sulaiman, A. Ma'Amor, N. M. Sarih, S. Mohamad, N.N.M. Zain, N.K. Abu Bakar and S. Mohamad, *Polymers (Basel)* **8**, 653 (2016). doi:10.3390/polym8050117.
- [8] M. Safarikova, I. Kibrikova, L. Ptackova, T. Hubka, K. Komarek, I. Safarik and J. Magn, *Magn. Mater* **293**, 377 (2005). doi:10.1016/j.jmmm.2005.02.034.

- [9] Z. Es'haghi and E. Esmaeili-Shahri, *J. Chromatogr. B* **973**, 142 (2014). doi:10.1016/j.jchromb.2014.09.030.
- [10] L.I. Abd Ali, W.A. Wan Ibrahim, A. Sulaiman, M.A. Kamboh and M.M. Sanagi, *Talanta* **148** (191) (2016). doi:10.1016/j.talanta.2015.10.062.
- [11] Y. Liu, Y. Wang, Q. Dai and Y. Zhou, *Anal. Chim. Acta* **936**, 168 (2016). doi:10.1016/j.aca.2016.07.003.
- [12] S.-K. Li, F.-Z. Huang, Y. Wang, Y.-H. Shen, L.-G. Qiu, A.-J. Xie and S.-J. Xu, *J. Mater. Chem.* **21**, 7459 (2011). doi:10.1039/c0jm04569a.
- [13] Q. Peng, Y. Liu, G. Zeng, W. Xu, C. Yang and J. Zhang, *J. Hazard. Mater.* **177**, 676 (2010). doi:10.1016/j.jhazmat.2009.12.084.
- [14] J. Ding, Q. Gao, D. Luo, Z.G. Shi and Y.Q. Feng, *J. Chromatogr. A* **1217**, 7351 (2010). doi:10.1016/j.chroma.2010.09.074.
- [15] E. Aliyari, M. Alvand and F. Shemirani, *RSC Adv.* **6**, 64193 (2016). doi:10.1039/C6RA04163A.
- [16] J.A. Rodriguez, J. Espinosa, K. Aguilar-Arteaga, I.S. Ibarra and J.M. Miranda, *Microchim. Acta* **171**, 407 (2010). doi:10.1007/s00604-010-0428-8.
- [17] I. Vasconcelos and C. Fernandes, *TrAC - Trends Anal. Chem.* **89**, 41 (2017). doi:10.1016/j.trac.2016.11.011.
- [18] K.M. Diniz and C.R.T. Tarley, *Microchem. J.* **123**, 185 (2015). doi:10.1016/j.microc.2015.06.011.
- [19] J. Ma, G. Wu, S. Li, W. Tan, X. Wang, J. Li and L. Chen, *J. Chromatogr. A* **1553**, 57 (2018). doi:10.1016/j.chroma.2018.04.034.
- [20] J. Ma, Z. Yao, L. Hou, W. Lu, Q. Yang, J. Li and L. Chen, *Talanta* **161**, 686 (2016). doi:10.1016/j.talanta.2016.09.035.
- [21] J. Ma, L. Jiang, G. Wu, Y. Xia, W. Lu, J. Li and L. Chen, *J. Chromatogr. A* **1466**, 12 (2016). doi:10.1016/j.chroma.2016.08.065.
- [22] J. Li, R. Dong, X. Wang, H. Xiong, S. Xu, D. Shen, X. Song and L. Chen, *RSC Adv.* **5**, 10611 (2015). doi:10.1039/C4RA11177J.
- [23] G. Wu, J. Ma, S. Li, J. Guan, B. Jiang, L. Wang, J. Li, X. Wang and L. Chen, *J. Colloid Interface Sci.* **528**, 360 (2018). doi:10.1016/j.jcis.2018.05.105.
- [24] A.R. Bagheri, M. Arabi, M. Ghaedi, A. Ostovan, X. Wang, J. Li and L. Chen, *Talanta* **195**, 390 (2019). doi:10.1016/j.talanta.2018.11.065.
- [25] X. Wu, X. Wang, W. Lu, X. Wang, J. Li, H. You, H. Xiong and L. Chen, *J. Chromatogr. A* **1435**, 30 (2016). doi:10.1016/j.chroma.2016.01.040.
- [26] W. Yang, T. Muhammad, A. Yigaimu, K. Muhammad and L. Chen, *J. Sep. Sci.* **41**, 4185 (2018). doi:10.1002/jssc.201800797.
- [27] P. Bera, C.H. Kim and S. Il Seok, *Polyhedron* **27**, 3433 (2008). doi:10.1016/j.poly.2008.07.039.
- [28] F.C. Lima, T.S. Silva, C.H.G. Martins and C.C. Gatto, *Inorganica Chim. Acta* **483**, 464 (2018). doi:10.1016/j.ica.2018.08.032.
- [29] X.-Y. Qiu, C. Zhang, S.-Z. Li, G.-X. Cao, P. Qu, F.-Q. Zhang, J.-G. Ma and B. Zhai, *Inorg. Chem. Commun.* **46**, 202 (2014). doi:10.1016/j.inoche.2014.05.015.
- [30] -F.N.-F. How, D.J. Watkin, K.A. Crouse, M.I.M. Tahir and A. Crystallogr, *Sect. E Struct. Reports Online* **63**, o3137 (2007). doi:10.1107/S1600536807024609.
- [31] M.T.H. Tarafder, A.M. Ali, Y.W. Wong, S.H. Wong and K.A. Crouse, *Synth. React. Inorg. Met. Chem.* **31**, 115 (2001). doi:10.1081/SIM-100001937.
- [32] M.T.H. Tarafder, K.-B. Chew, K.A. Crouse, A.M. Ali, B.M. Yamin and H.-K. Fun, *Polyhedron* **21**, 2683 (2002). doi:10.1016/S0277-5387(02)01285-8.
- [33] E. Zangrando, M.T. Islam, M.A.A.A. Islam, M.C. Sheikh, M.T.H. Tarafder, R. Miyatake, R. Zahan and M.A. Hossain, *Inorganica Chim. Acta* **427** (278) (2015). doi:10.1016/j.ica.2014.12.014.
- [34] M.S. Begum, E. Zangrando, M.B.H. Howlader, M.C. Sheikh, R. Miyatake, M.M. Hossain, M. M. Alam and M.A. Hasnat, *Polyhedron*. **105** (56) (2016). doi:10.1016/j.poly.2015.11.046.
- [35] R. Takjoo, R. Centore and S.S. Hayatolghaibi, *Inorganica Chim. Acta* **471** (587) (2018). doi:10.1016/j.ica.2017.11.043.
- [36] D.Z. Wang, S.F. Zhang, Y. Zhang and L. Lin, *J. Proteomics.* **132–140**, 135 (2016).
- [37] E.N.M. Yusof, T.B.S.A. Ravoof, J. Jamsari, E.R.T. Tiekink, A. Veerakumarasivam, K.A. Crouse, M.I. M. Tahir and H. Ahmad, *Inorganica Chim. Acta* **438**, 85 (2015). doi:10.1016/j.ica.2015.08.029.

- [38] -F.N.-F. How, K.A. Crouse, M.I.M. Tahir, M.T.H. Tarafder and A.R. Cowley, *Polyhedron* **27**, 3325 (2008). doi:10.1016/j.poly.2008.07.022.
- [39] A.B. Rode, J. Kim, S.-H. Kim, G. Gupta and I.S. Hong, *Tetrahedron Lett.* **53**, 2571 (2012). doi:10.1016/j.tetlet.2012.03.040.
- [40] H.R. Rajabi, H. Arjmand, S.J. Hoseini, H. Nasrabadi and J. Magn, *Magn. Mater* **394**, 7 (2015). doi:10.1016/j.jmmm.2015.06.024.
- [41] A. Mohammadi, M. Barikani and M.M. Lakouraj, *Mater. Sci. Eng. C* **66**, 106 (2016). doi:10.1016/j.msec.2016.04.064.
- [42] E.N.M. Yusof, N.M. Nasri, T.B.S.A. Ravoof and E.R.T. Tiekink, *Molbank*. **2019**, 2 (2019).
- [43] R.A. Bhat and D. Kumar, *Res. Chem. Intermed.* **45**, 2565 (2019). doi:10.1007/s11164-019-03752-0.
- [44] A. Liopo, R. Su and A.A. Oraevsky, *Photoacoustics* **3** (35) (2015). doi:10.1016/j.pacs.2015.02.001.
- [45] S. Sinniah, S. Mohamad and N.S.A. Manan, *Appl. Surf. Sci.* **357**, 543 (2015). doi:10.1016/j.apsusc.2015.09.078.
- [46] G. Giakisikli and A.N. Anthemidis, *Anal. Chim. Acta* **789**, 1 (2013). doi:10.1016/j.aca.2013.04.021.
- [47] Z.Y. Ma, Y.P. Guan, X.Q. Liu and H.Z. Liu, *J. Appl. Polym. Sci.* **96**, 2174 (2005). doi:10.1002/app.21688.
- [48] K.C. de Souza, G.F. Andrade, I. Vasconcelos, I.M. de Oliveira Viana, C. Fernandes and E.M.B. de Sousa, *Mater. Sci. Eng. C* **40**, 275 (2014). doi:10.1016/j.msec.2014.04.004.
- [49] E. Alzahrani, *Int. J. Anal. Chem.* **2015** (2015). doi:10.1155/2015/797606
- [50] W. Wu, Q. He and C. Jiang, *Nanoscale Res. Lett.* **3**, 397 (2008).
- [51] S.R. Chowdhury, E.K. Yanful and A.R. Pratt, *J. Hazard. Mater* **235–236**, 246 (2012). doi:10.1016/j.jhazmat.2012.07.054.
- [52] M.A. Ahmed, S.M. Ali, S.I. El-Dek and A. Galal, *Mater. Sci. Eng. B* **178**, 744 (2013). doi:10.1016/j.mseb.2013.03.011.
- [53] S. Rajput, C.U. Pittman and D. Mohan, *Colloid Interface Sci.* **468**, 334 (2016). doi:10.1016/j.jcis.2015.12.008.
- [54] M.H. Mashhadizadeh, M. Pesteh, M. Talakesh, I. Sheikhshoae, M.M. Ardakani and M.A. Karimi, *Spectrochim. Acta - Part B At. Spectrosc.* **63**, 885 (2008). doi:10.1016/j.sab.2008.03.018.
- [55] K. Alizadeh, R. Parooi, P. Hashemi, B. Rezaei and M.R. Ganjali, *J. Hazard. Mater* **186**, 1794 (2011). doi:10.1016/j.jhazmat.2010.12.067.
- [56] H. Bagheri, A. Afkhami, M. Saber-Tehrani and H. Khoshsafar, *Talanta* **97** (87) (2012). doi:10.1016/j.talanta.2012.03.066.
- [57] G. Cheng, M. He, H. Peng and B. Hu, *Talanta* **88** (507) (2012). doi:10.1016/j.talanta.2011.11.025.
- [58] A.E. Karatapanis, Y. Fiamegos and C.D. Stalikas, *Talanta* **84** (834) (2011). doi:10.1016/j.talanta.2011.02.013.
- [59] A.B. Tabrizi, M.R. Rashidi and H. Ostadi, *J. Braz. Chem. Soc.* **25**, 709 (2014).
- [60] S.P. Mishra, *Curr. Sci.* **107**, 601 (2014).
- [61] W.J. Chen, L.C. Hsiao and K.K.Y. Chen, *Process Biochem.* **43**, 488 (2008). doi:10.1016/j.procbio.2007.11.017.
- [62] Y. Çağlar, E.T. Saka and J. Karbala *Int. Mod. Sci.* **3**, 185 (2017).
- [63] Q. Chang, J. Zhang, X. Du, J. Ma and J. Li, *Front. Environ. Sci. Eng. China* **4**, 187 (2010). doi:10.1007/s11783-010-0030-7.
- [64] G. Vatankhah, M. Ebrahimi and M. Kahani, *Eurasian J. Anal. Chem.* **12**, 987 (2017). doi:10.12973/ejac.2017.00227a.
- [65] B. Topuz, F. Kabadayi and A. Solmaz, *Int. J. Environ. Anal. Chem.* **99**, 641 (2019). doi:10.1080/03067319.2019.1607317.
- [66] L. Meira, J. Almeida, F. Dias and L. Teixeira, *Brazilian J. Anal. Chem.* 60–66, **6** (2019).